

## Electronic Supplementary Information

# Functional Porous Composites by Blending with Solution-Processable Molecular Pores

S. Jiang, L. Chen, M. E. Briggs, T. Hasell and A. I. Cooper\*

Department of Chemistry, University of Liverpool, Liverpool L69 7ZD, UK

### Table of contents

#### 1. Experimental

Table S1. Synthesis of cage-pyrene composites with various pyrene loading

Table S2. Synthesis of cage-polymer composites with various polymer loading

#### 2. Characterisation and Analysis

Figure S1. MALDI-TOF data for scrambled cages.

Figure S2. Powder XRD patterns for crystalline pyrene, amorphous scrambled cages, and cage-pyrene composites at various pyrene loading.

Figure S3. SEM images for pyrene (a), scrambled cages (b), and cage-pyrene composite with 16 wt.% pyrene loading (c).

Figure S4. (a) <sup>1</sup>H-NMR spectra of scrambled cages (black), pyrene (red), and cage-pyrene composite with 16 wt.% pyrene loading (blue). (b) An enlarged view of chemical shift between 7.8 and 8.4 for pyrene. The peaks are assigned to the protons on aromatic rings of pyrene.

Figure S5. <sup>1</sup>H-NMR spectrum of cage-pyrene composite with 16 wt.% pyrene loading

Figure S6. FTIR spectra for pyrene (black), scrambled cages (red) and cage-pyrene composite with 16 wt.% pyrene loading (blue).

Figure S7. Images of scramble cages (a) and cage-pyrene composite with 16 wt.% pyrene (b) under UV light with a wavelength of 254 nm.

Figure S8. The pyrene excimer/monomer (*e/m*) ratio in the composites plotted as function of the pyrene loading.

Table S3. BET surface areas, N<sub>2</sub> uptakes and pore volumes comparison between scrambled cages, pyrene, and cage-pyrene composites with a various pyrene loading.

Figure S9. CO<sub>2</sub> adsorption and desorption at 298 K for scrambled cages and cage-pyrene composites with a various pyrene loading.

Figure S10. BET surface areas for the cage-polymer composites measured by Quantachrome gas sorption instrument with a different polymer loading. The polymers include PMMA, PVP, PEI and PS.

Figure S11. <sup>1</sup>H-NMR spectra of scrambled cages (black), PEI (red) and cage-PEI composite with 33 wt.% PEI loading (blue)

Figure S12. <sup>1</sup>H-NMR spectrum of cage-PEI composite with 33 wt.% PEI loading

Figure S13. FTIR spectra for scrambled cages (black), PEI (red) and cage-PEI composite with 23 wt.% PEI loading (blue).

Figure S14: TGA analysis for PEI (black curve), amorphous scrambled cages (red curve), and cage-PEI composites at various PEI loading.

Figure S15. Powder XRD patterns for PEI, amorphous scrambled cages, and cage-PEI composites at various PEI loading.

Table S4. BET surface areas, N<sub>2</sub> uptakes, and pore volumes comparison between scrambled cages, PEI and cage-PEI composites with a various PEI loading.

## Experimental

**Materials.** 1,3,5-Triformylbenzene was purchased from Manchester Organics, (1*R*,2*R*)-(-)-1,2-cyclohexanediamine was purchased from TCI-UK. 1,2-Diaminoethane, pyrene, polymers were purchased from Sigma Aldrich. All other chemicals were purchased from Fisher and used as received.

### Synthesis of scrambled cages

The synthetic procedure has been described in the previous study.<sup>[1]</sup> Dichloromethane (DCM, 400 mL) was added to 1,3,5-triformylbenzene (5 g, 30.9 mmol) in a round flask at room temperature. A solution of 1,2-diaminoethane (0.9 g, 15.4 mmol) in DCM (200 mL) and a solution of (1*R*,2*R*)-(-)-1,2-cyclohexanediamine (3.5 g, 30.9 mmol) in DCM (200 mL) were slowly added sequentially. After complete addition, the reaction was allowed to stir for 2–3 days at room temperature. A clear homogeneous solution was observed with no undissolved material being present. The reaction mixture was concentrated on a rotary evaporator, triturated with ethyl acetate then isolated by filtration to remove any unreacted starting materials. The product was vacuum dried overnight before analysis. Typical yield after washing = 70–75 %.

### Synthesis of cage-pyrene composites

The scrambled cages (100 mg) were dissolved in DCM (20 mL) in a sample vial at room temperature. A stock solution of pyrene in DCM (10 mg/mL) was made. The corresponding pyrene solution was added into the scrambled cages solution to form composites. The four cage-pyrene composites were prepared with a pyrene loading at 3 wt.%, 5 wt.%, 10 wt.%, and 15 wt.%, respectively. The amounts are listed in table S1. The mixed solution was stirred for a day. The products were obtained by evaporating the solvents using the rotary evaporator. Accurate pyrene loading was verified by <sup>1</sup>H-NMR and was consistent with the expected 3 wt.%, 6 wt.%, 10 wt.%, or 16 wt.% loadings.

Table S1. Synthesis of cage-pyrene composites with various pyrene loading.

	Mass of scrambled cages in composite material	Volume of pyrene stock solution in composite material (10 mg/ml)
3 wt.% pyrene loading	100 mg	0.3 ml
5 wt.% pyrene loading	100 mg	0.5 ml
10 wt.% pyrene loading	100 mg	1.1 ml
15 wt.% pyrene loading	100 mg	1.8 ml

**High throughput preparation of samples for surface area screening:**

Stock solutions of polymers (polyethyleneimine (PEI) ( $M_n = 5000$ ), polyvinylpyrrolidone (PVP) ( $M_n = 360k$ ), poly(methyl methacrylate) (PMMA) ( $M_n = 15k$ ), and polystyrene (PS) ( $M_n = 192k$ ) and scramble cages were made at a concentration of 10 mg/mL in DCM. The solutions were dispensed into the sample vials using a robotic dispensing instrument (Eppendorf epMotion 5075PC). The amounts were listed in Table S2. The mixed solutions were stirred on the robot deck for 1–2 hours and the composites products were obtained by freeze drying. The cage-polymer composites with polymer loading 5, 10, 15, 20, 30, 40, 60 and 80 wt.% were prepared..

Table S2. Synthesis of cage-polymer composites with various polymer loadings

wt.%	Volume of polymer solution/mL	Volume of polymer solution/mL
5	0.5	9.5
10	1	9
15	1.5	8.5
20	2	8
30	3	7
40	4	6
60	6	4
80	8	2

### Synthesis of cage-PEI composites

Linear PEI ( $M_n = 5000$   $PDI < 1.2$ ) was used. Due to its hydroscopic properties, PEI was handled in a glove box.

The scrambled cages (100 mg) were dissolved in DCM (20 mL) in a round-bottomed flask at room temperature. A stock solution of linear PEI in MeOH was prepared with a concentration of 10 mg/mL. Five cage-PEI composites samples at different PEI loadings were prepared, corresponding to 5 wt.%, 10 wt.%, 15 wt.%, 20 wt.%, and 30 wt.%. The mixed solution was stirred for a day. The composites materials were obtained by evaporating the solvents using the freeze drying. The samples were vacuumed dried overnight before analysis. The PEI loading calculated from NMR was 5 wt.%, 9 wt.%, 17 wt.%, 23 wt.%, 3 and 3 wt.%.

## Characterization and Analysis

**Nuclear Magnetic Resonance (NMR) Spectroscopy.** Solution  $^1\text{H}$  NMR spectra were recorded at 400.13 MHz using a Bruker Avance 400 NMR spectrometer.

**Fourier Transform Infrared Spectroscopy (FTIR).** IR spectra were recorded using a Bruker Tensor 27 FT-IR spectrometer with Quest ATR (diamond crystal puck) attachment running Opus 6.5 software. Samples were analysed as dry powders for 16 scans with a resolution of  $4\text{ cm}^{-1}$ . Spectra were recorded in transmission mode.

**Thermogravimetric Analysis (TGA).** TGA analysis was carried out using a Q5000IR analyzer (TA instruments) with an automated vertical overhead thermobalance. The samples were heated at the rate of  $5\text{ }^\circ\text{C}/\text{min}$ .

**Analytical HPLC.** HPLC data was obtained using a Dionex UltiMate 3000 system. The column used for the analysis of scrambled cages was a Synchronis C8,  $150 \times 4.6\text{ mm}$ ,  $3\text{ }\mu\text{m}$  (97203-154630, 12475). The mobile phase was methanol at a flow rate of  $1\text{ mL}/\text{min}$ . The column oven temperature was set to  $30\text{ }^\circ\text{C}$ . Detection for HPLC analysis was conducted at  $254\text{ nm}$ .

**Powder X-ray Diffraction.** Powder X-ray diffraction data were collected on a Panalytical X'pert pro multi-purpose diffractometer in transmission Debye-Scherrer geometry operating with a Cu anode at  $40\text{ kV}$   $40\text{ mA}$ . Samples were ground and mounted as loose powder onto a transparent film and spun at  $2\text{ s}/\text{rotation}$ . PXRD patterns were collected in two 1-h scans with a step size of  $0.013^\circ 2\theta$  and scan time of  $115\text{ s}/\text{step}$  over  $5\text{--}50^\circ 2\theta$ . The incident X-ray beam was conditioned with  $0.04\text{ rad}$  Soller slits and an anti-scatter slit of  $1/2^\circ$ . The diffracted beam passed through an automatic antiscatter slit ( $5\text{ mm}$ ),  $0.04\text{ rad}$  Soller slits and Ni filter before processing by the PIXcel detector operating in scanning mode.

**Scanning electron microscopy (SEM).** High resolution imaging of the morphology was achieved using a Hitachi S-4800 cold Field Emission Scanning Electron Microscope (Hitachi). The dry samples were prepared on  $15\text{ mm}$  Hitachi M4 aluminium stubs using an adhesive high purity carbon tab. The samples were then coated with a  $2\text{ nm}$  layer of gold

using an Emitech K550X automated sputter coater. The field emission scanning electron microscope measurement scale bar was calibrated against certified standards. Imaging was conducted at a working distance of 8 mm and a working voltage of 3 kV using a mix of upper and lower secondary electron detectors.

**Gas Sorption Analysis.** All samples were tested with gases of the following purities: hydrogen (99.9995%, BOC gases), carbon dioxide (SCF grade, BOC gases) and methane (ultrahigh purity, BOC gases). Most surface areas and pore size distributions were measured by nitrogen adsorption and desorption at 77.3 K using a Micromeritics ASAP 2020 volumetric adsorption analyzer. Samples were degassed at offline at 60 °C for 15 h under dynamic vacuum ( $10^{-5}$  bar) before analysis, followed by degassing on the analysis port, also at 80 °C. Carbon dioxide isotherms were measured at 273 and 293 K using a Micromeritics 2020 volumetric adsorption analyzer using the same degassing procedure. High throughput samples were measured for 5-point BET on Quantachrome Nova 4200 Surface Area Analyzers running in parallel, with 4 sorption ports each. Samples were run at 77 K, after degassing at 90 °C for 12 h under dynamic vacuum.

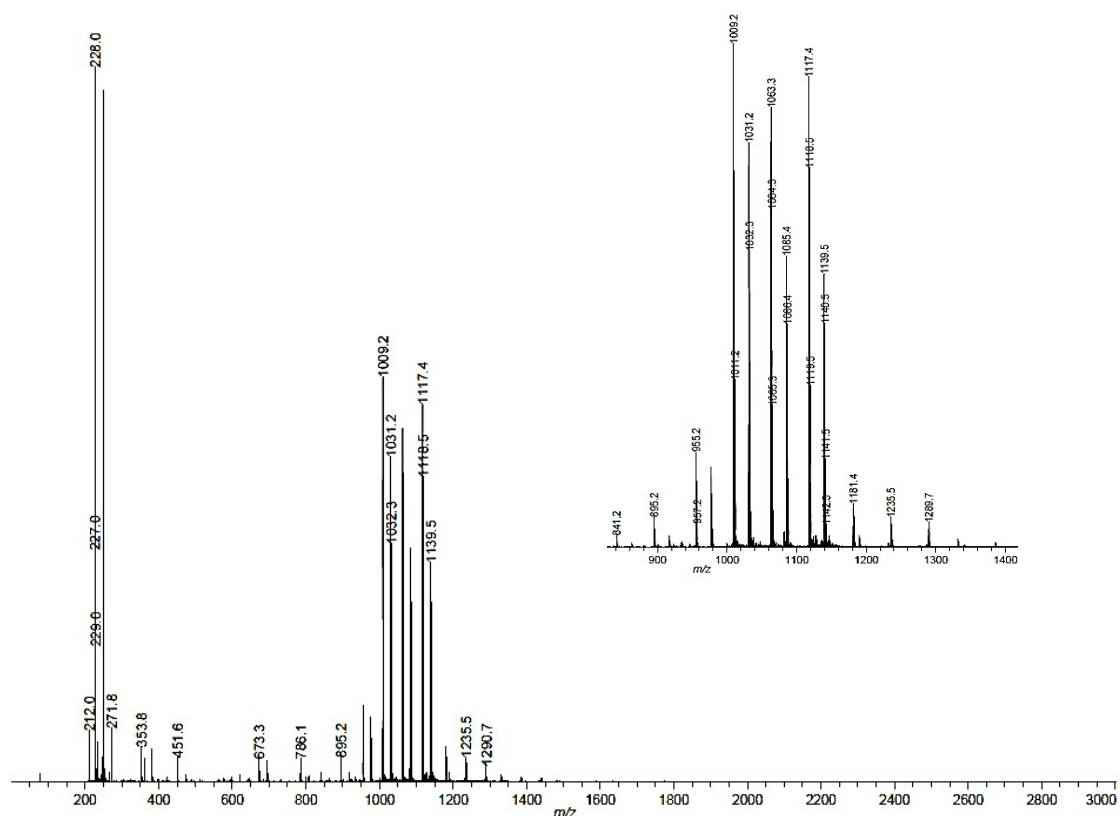


Figure S1. MALDI-TOF data for scrambled cages. An enlarged view of  $m/z$  ratios between 900 and 1400 is concluded.

Calculated for **CC1**, **CC1<sup>531</sup>**, **CC1<sup>432</sup>**, **CC1<sup>333</sup>**, **CC1<sup>234</sup>**, **CC1<sup>135</sup>**, and **CC3**: 792, 846, 900, 954, 1008, 1062, and 1116, respectively.  $m/z$  ratios correspond to 955 [**CC1<sup>333</sup>+H**]<sup>+</sup>, 1009 [**CC1<sup>234</sup>+H**]<sup>+</sup>, 1031 [**CC1<sup>234</sup>+Na**]<sup>+</sup>, 1063 [**CC1<sup>135</sup>+H**]<sup>+</sup>, 1085 [**CC1<sup>135</sup>+Na**]<sup>+</sup>, 1117 [**CC3+H**]<sup>+</sup>, 1139 [**CC3+Na**]<sup>+</sup>, 1181 [**CC1<sup>333</sup>+Dithranol**]<sup>+</sup>, 1235 [**CC1<sup>234</sup>+Dithranol**]<sup>+</sup> and 1289 [**CC1<sup>135</sup>+Dithranol**]<sup>+</sup>. Dithranol, THF and NaI are the matrix for MALDI-TOF analysis.



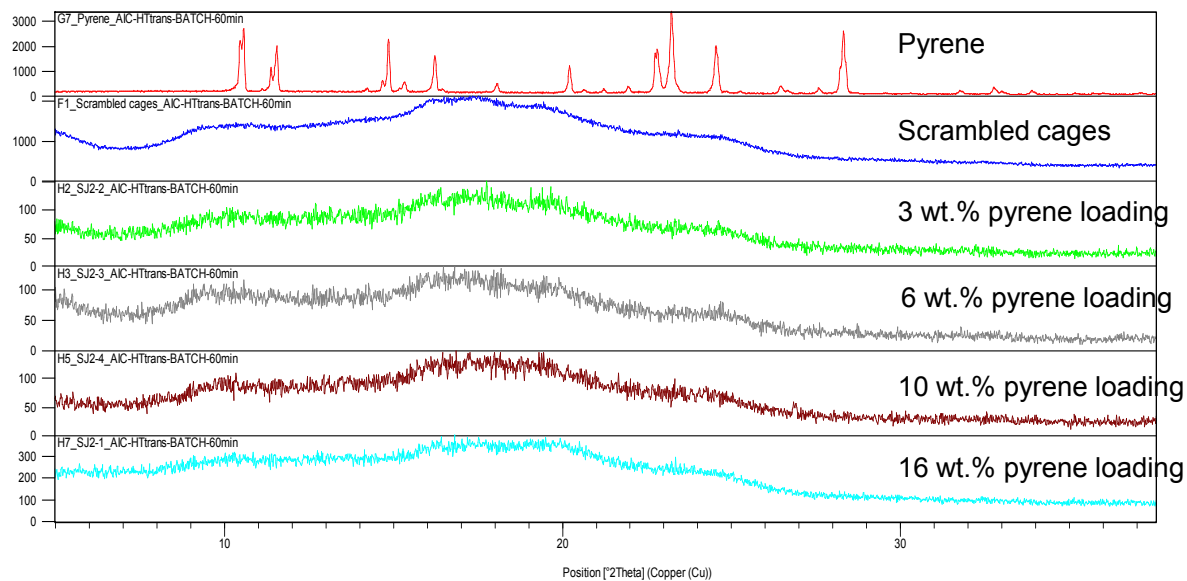


Figure S2. Powder XRD patterns for crystalline pyrene, amorphous scrambled cages, and cage-pyrene composites at various pyrene loading. The composite materials show amorphous phases.

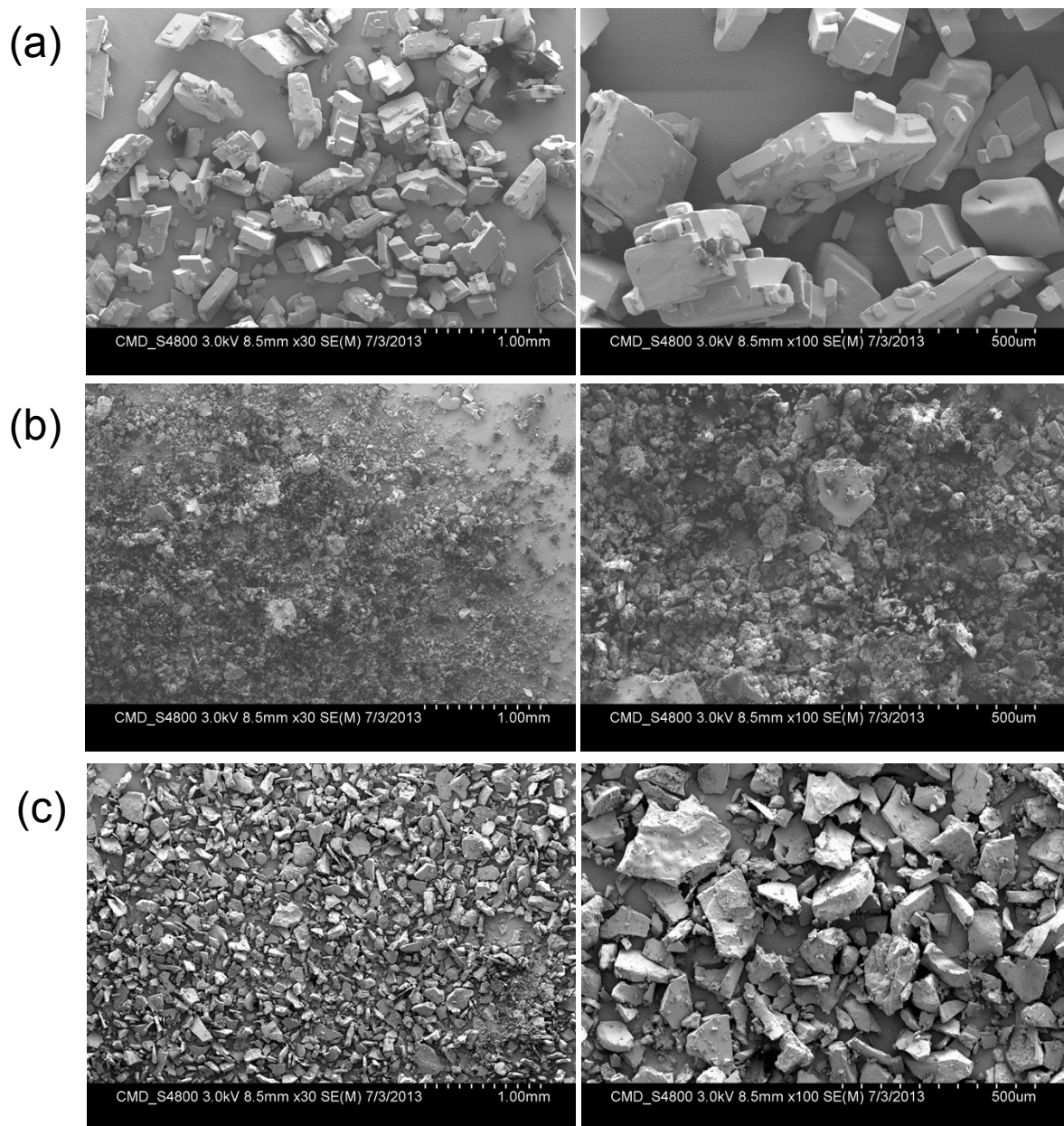


Figure S3. SEM images for pure pyrene (a), pure scrambled cages (b) and a cage-pyrene composite with 16 wt.% pyrene loading (c).

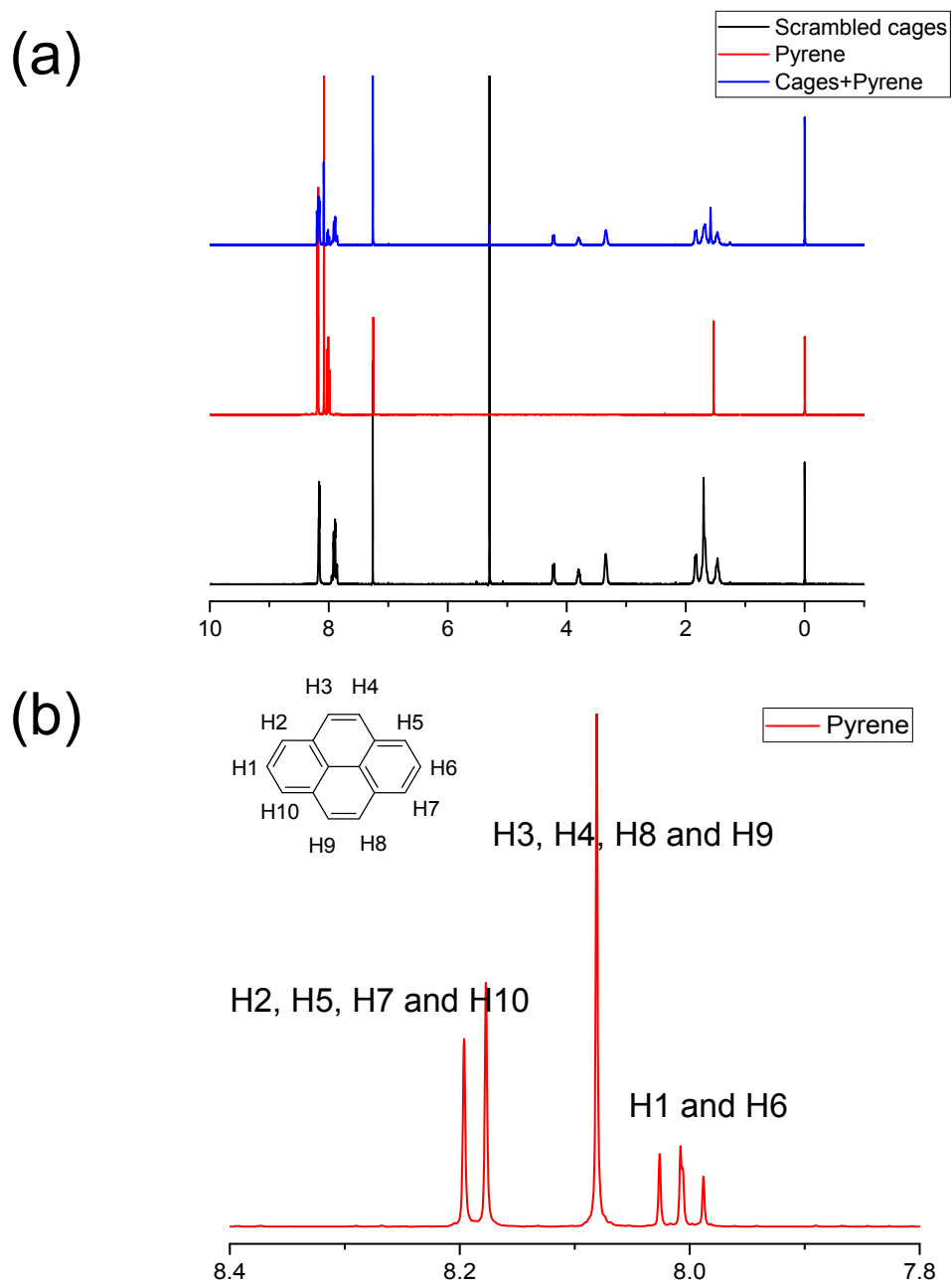


Figure S4. (a)  $^1\text{H}$ -NMR spectra of scrambled cages (black), pyrene (red) and cage-pyrene composite with 16 wt.% pyrene loading (blue). (b) An enlarged view of chemical shift between 7.8 and 8.4 for pyrene. The peaks are assigned to the protons on aromatic rings of pyrene.

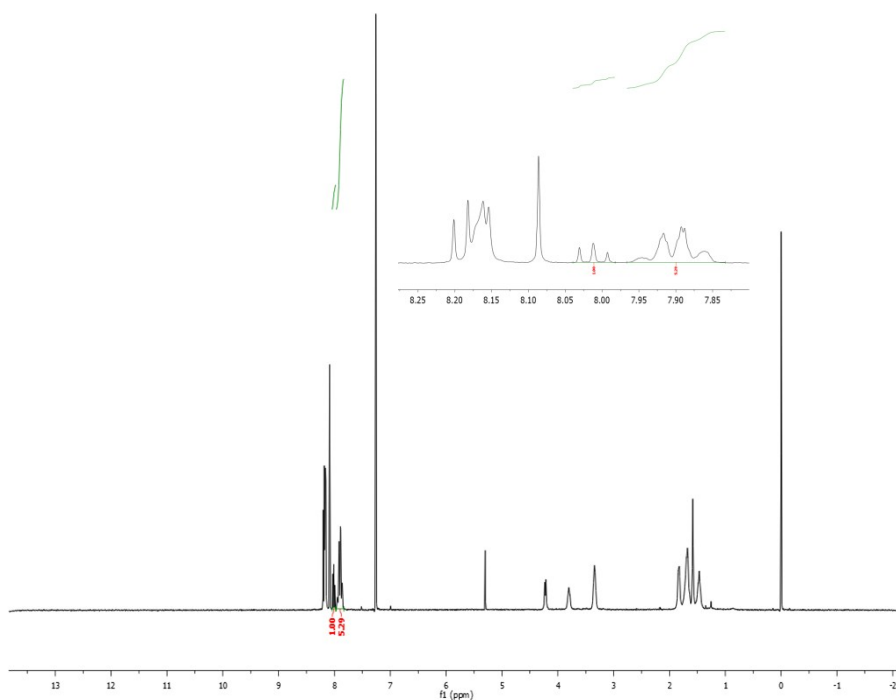


Figure S5. <sup>1</sup>H-NMR spectra of cage-pyrene composite with 16 wt.% pyrene loading. The triplet peaks at ~ 8.02 ppm are assigned to the protons on aromatic rings of pyrene with 2H. The multiple peaks at ~ 7.9 ppm are consistent with protons on aromatic rings of scrambled cages with 12H. The integration of the peak area at ~8.02 ppm is 1, compared with 0.53 of the integration of the peak area ~7.9 ppm. The accurate pyrene loading can be calculated by the integrations of two peak areas.

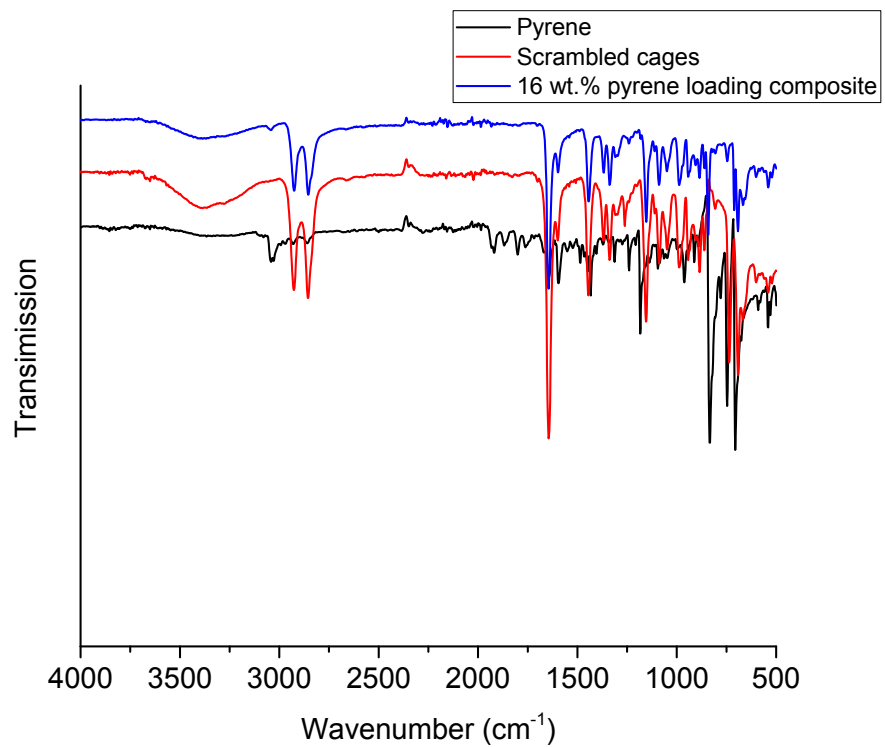


Figure S6. FTIR spectra for pyrene (black), scrambled cages (red) and cage-pyrene composite with 16 wt.% pyrene loading (blue).

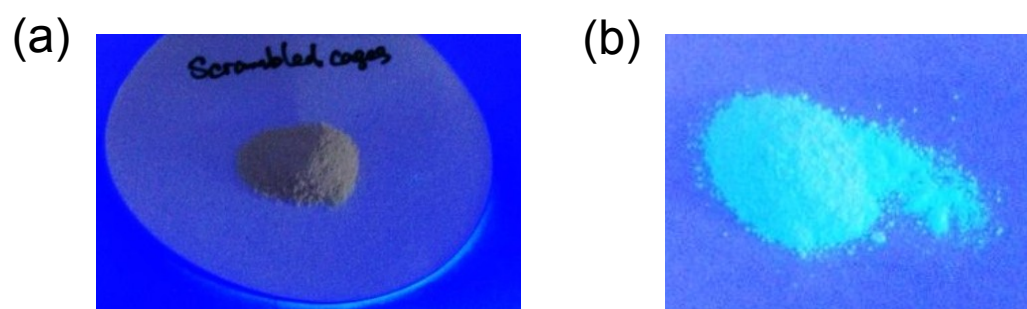


Figure S7. Images of scramble cages (a) and cage-pyrene composite with 16 wt.% pyrene (b) under UV light with a wavelength of 254 nm.

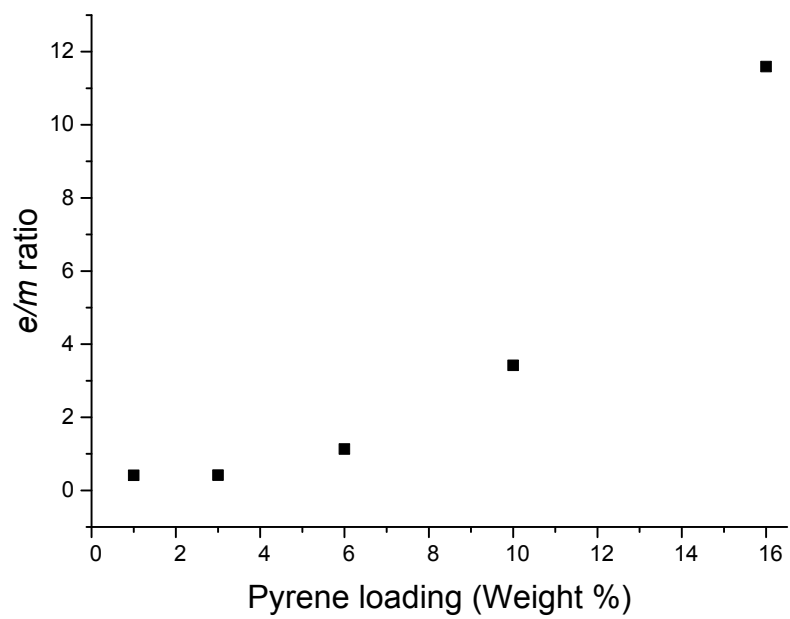


Figure S8. The pyrene excimer/monomer ( $e/m$ ) ratio in the composites plotted as function of the pyrene loading. The  $e/m$  ratio was calculated by comparing the fluorescence intensity of the excimer band at 470 nm to the first monomer peak at 373 nm.

	BET Surface areas (m <sup>2</sup> g <sup>-1</sup> )	N <sub>2</sub> uptakes (mmol g <sup>-1</sup> ) (1 bar, 77 K)	t-plot pore volumes (cm <sup>3</sup> g <sup>-1</sup> )
Scrambled cages	718	11.29	0.26
Pyrene	N/A	0.26	N/A
Composites with 3 wt.% pyrene loading	635	9.14	0.23
Composites with 6 wt.% pyrene loading	513	7.98	0.19
Composites with 10 wt.% pyrene loading	197	3.02	0.076
Composites with 16 wt.% pyrene loading	N/A	0.83	N/A

Table S3. Apparent BET surface areas, N<sub>2</sub> uptakes and pore volumes comparison between scrambled cages, pyrene and cage-pyrene composites with various pyrene loading.



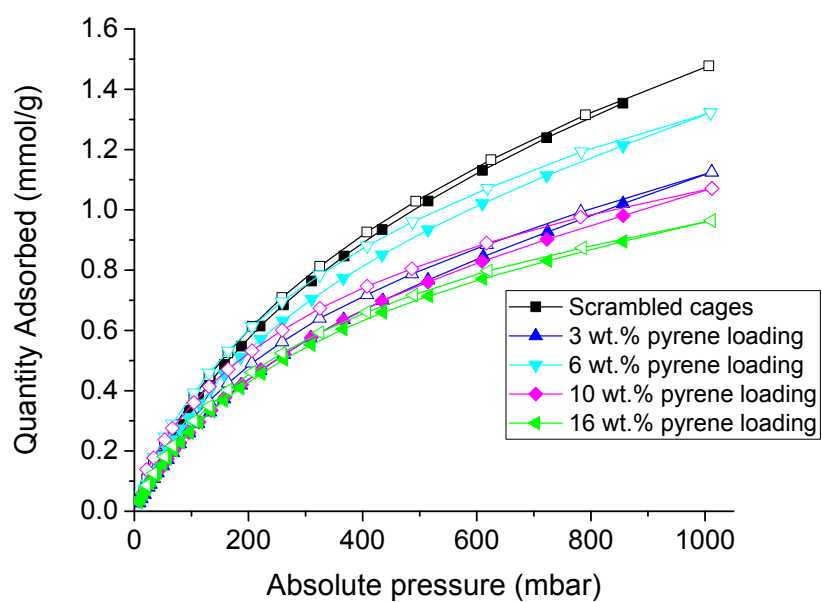


Figure S9. CO<sub>2</sub> adsorption and desorption at 298 K for scrambled cages and cage-pyrene composites with a various pyrene loading.

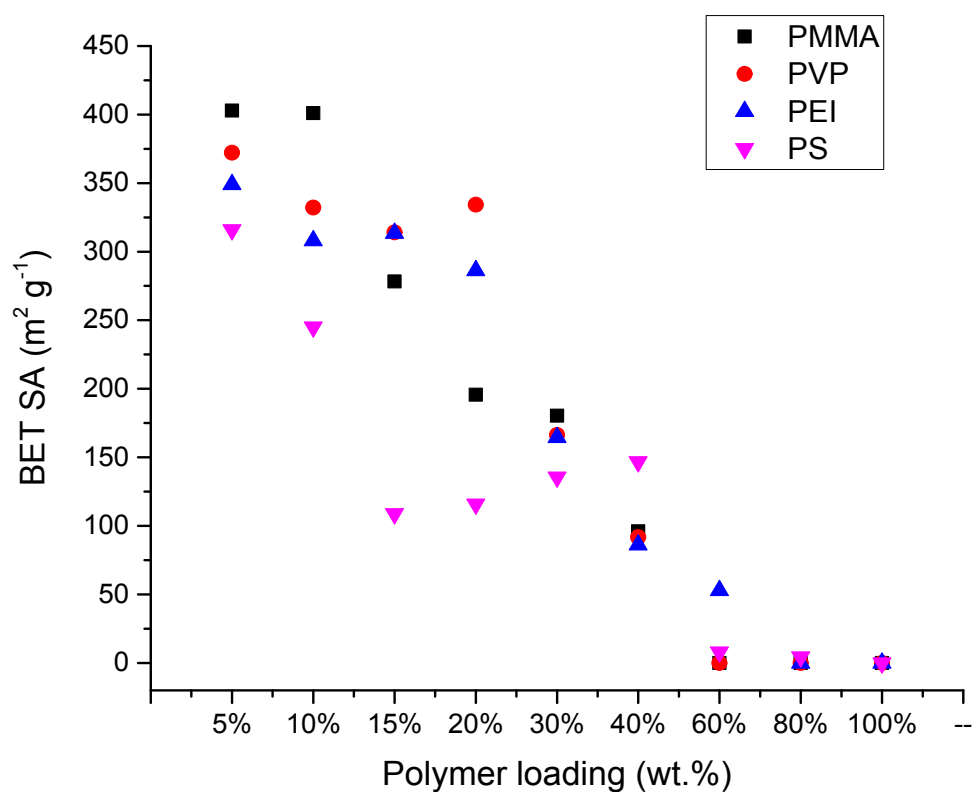


Figure S10. BET surface areas for the cage-polymer composites measured using a Quantachrome gas sorption instrument with a different polymer loading. The polymers include poly(methyl methacrylate) (PMMA), polyvinylpyrrolidone (PVP), polyethyleneimine (PEI) and polystyrene (PS).

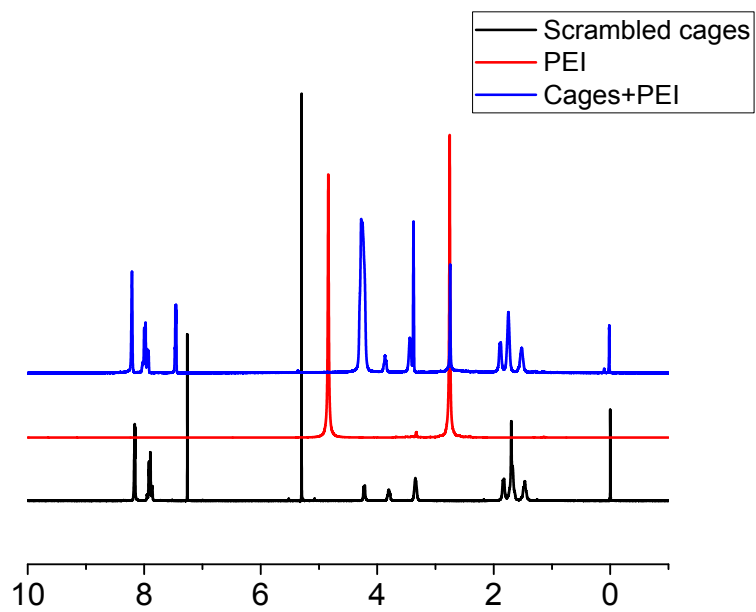


Figure S11. <sup>1</sup>H-NMR spectra of scrambled cages (black), PEI (red) and cage-PEI composite with 33 wt.% PEI loading (blue).

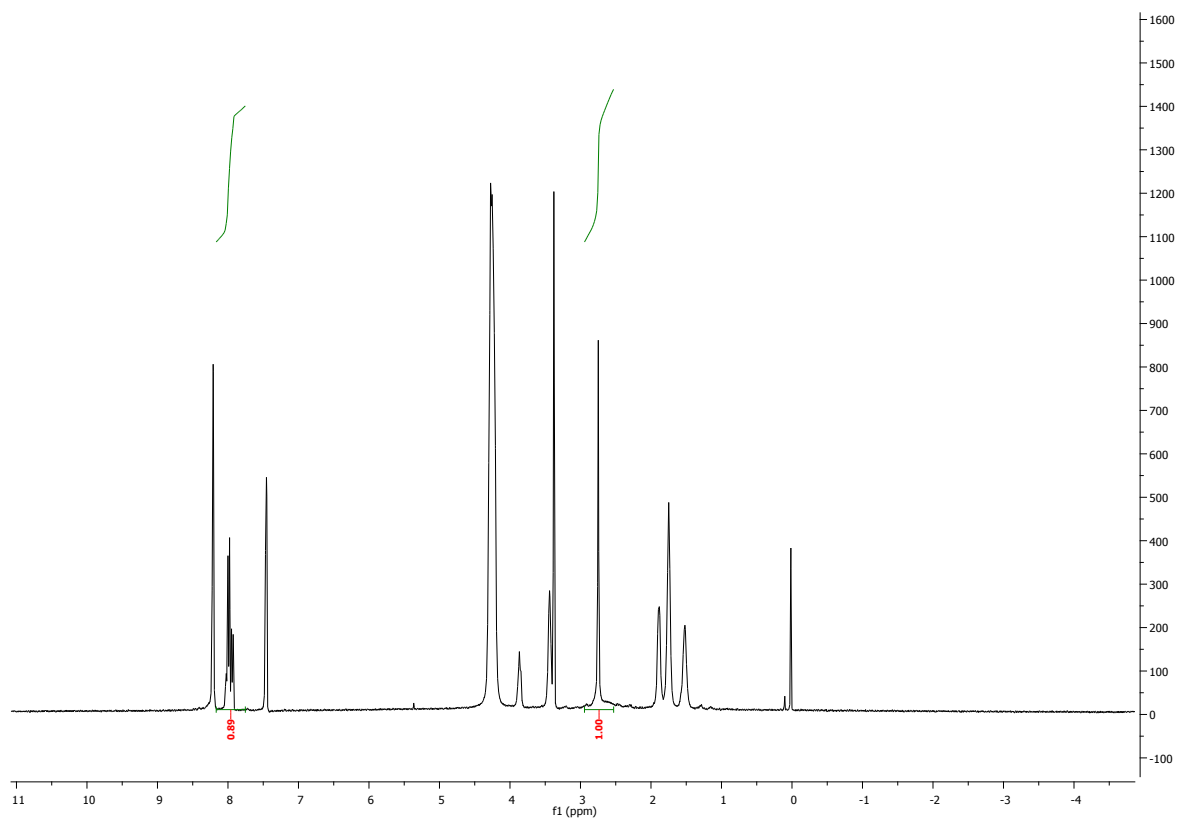


Figure S12.  $^1\text{H}$ -NMR spectra of cage-PEI composite with 33 wt.% PEI loading. The peak at 2.73 ppm is assigned to the protons of the linear PEI backbone  $\text{N-CH}_2$ . The multiple peaks at  $\sim 7.9$  ppm are consistent with protons on aromatic rings of scrambled cages with 12H. The accurate PEI loading can be calculated by the integrations of two peak areas.

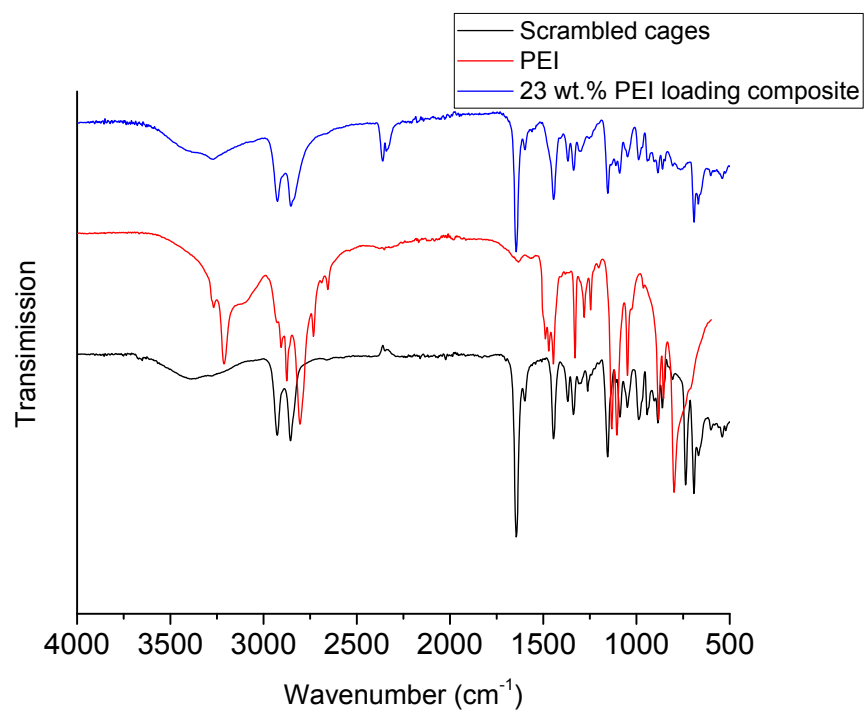


Figure S13. FTIR spectra for scrambled cages (black), PEI (red) and cage-PEI composite with 23 wt.% PEI loading (blue).

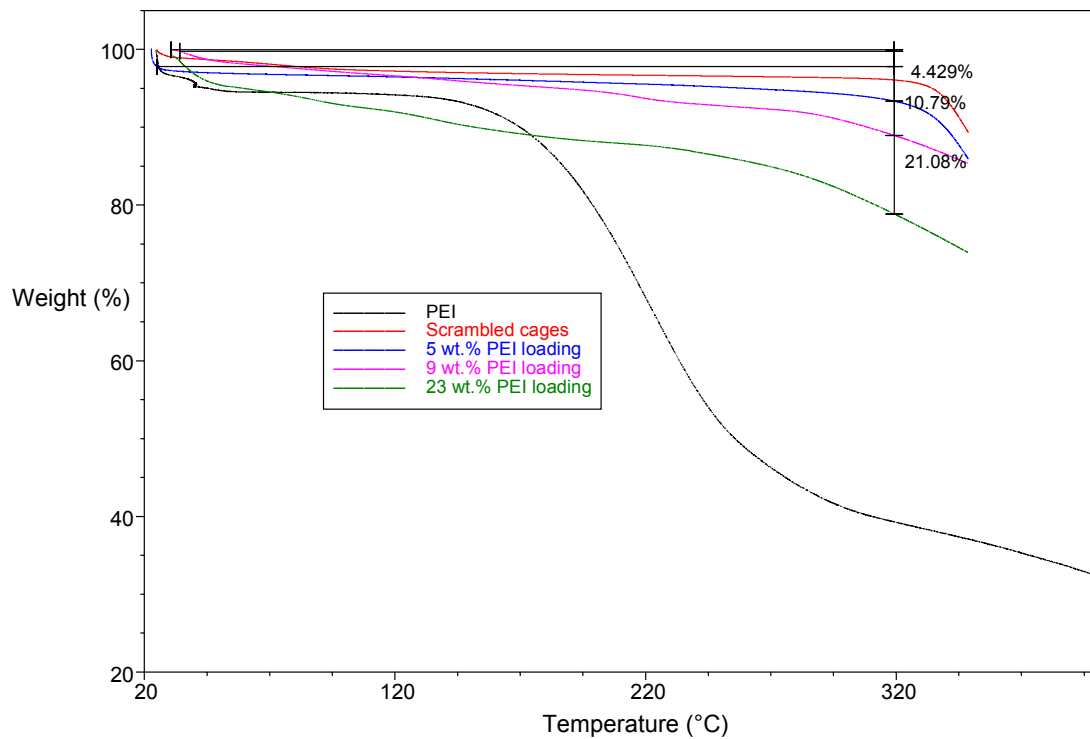


Figure S14: TGA analysis for PEI (black curve), amorphous scrambled cages (red curve), and cage-PEI composites at various PEI loading. The weight loss at 320 °C agrees with the amount of PEI loading.

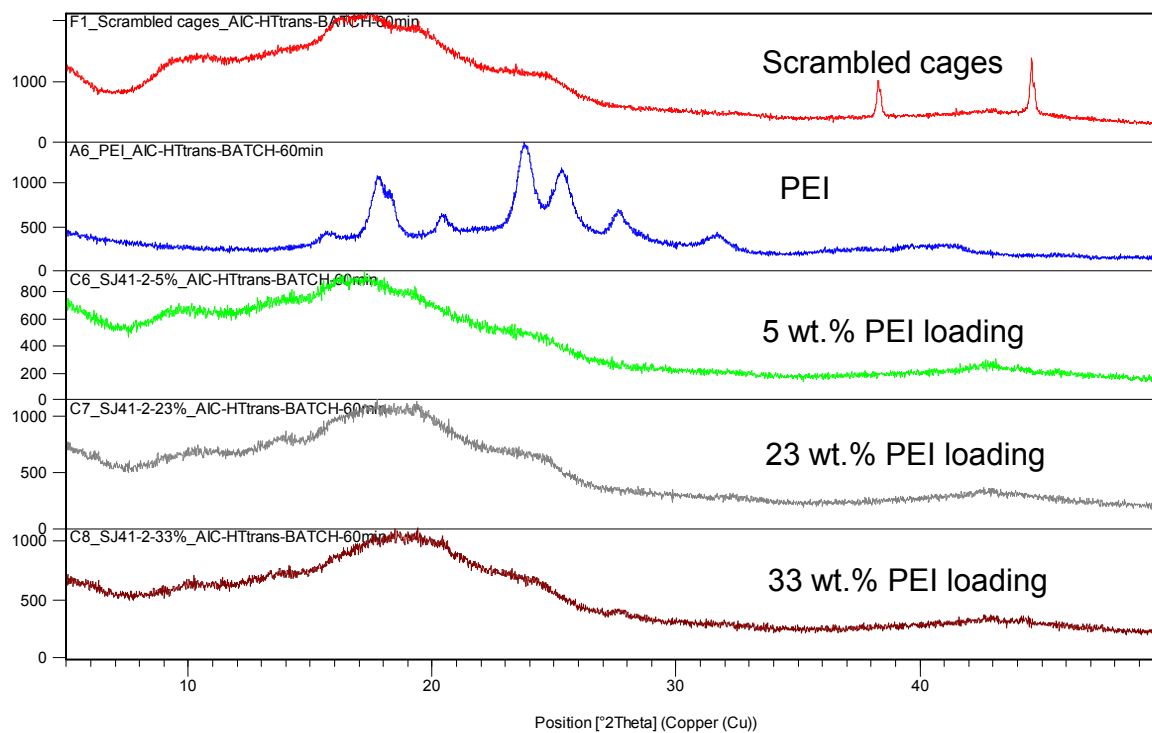


Figure S15. Powder XRD patterns for PEI, amorphous scrambled cages, and cage-PEI composites at various PEI loading. The composite materials show amorphous phases. The peaks shown for scrambled cages at  $38^\circ$  and  $45^\circ$  correspond to the aluminium of the sample holder.

	BET Surface areas (m <sup>2</sup> g <sup>-1</sup> )	N <sub>2</sub> uptakes (77 K) (mmol g <sup>-1</sup> )	CO <sub>2</sub> uptakes (1.2 bar 298 K) (mmol g <sup>-1</sup> )	Micropore volumes (cm <sup>3</sup> g <sup>-1</sup> )
Scrambled cages	718	11.26	1.48	0.26
PEI	N/A	N/A	1.47	N/A
Composites with 5 wt.% PEI loading	540	9.90	1.93	0.22
Composites with 9 wt.% PEI loading	496	8.98	1.93	0.20
Composites with 17 wt.% PEI loading	250	4.98	2.08	0.092
Composites with 23 wt.% PEI loading	215	4.26	1.95	0.077
Composites with 33 wt.% PEI loading	164	3.21	1.86	0.064

Table S4. BET surface areas, N<sub>2</sub> uptakes and pore volumes comparison between scrambled cages, PEI and cage-PEI composites with a various PEI loading.

Reference:

- [1] S. Jiang, J. T. A. Jones, T. Hasell, C. E. Blythe, D. J. Adams, A. Trewin and A. I. Cooper, *Nat. Commun.*, 2011, **2**, 207.